THE ASTROPHYSICAL JOURNAL, 452:230–237, 1995 October 10


# TESTING UNIFIED X-RAY/ULTRAVIOLET ABSORBER MODELS WITH NGC 5548

SMITA MATHUR, MARTIN ELVIS, AND BELINDA WILKES
Harvard-Smithsonian Center for Astrophysics, 60 Garden Street, Cambridge, MA 02138; smita@cfa.harvard.edu
*Received 1995 February 21; accepted 1995 April 21*

## ABSTRACT

The bright Seyfert galaxy NGC 5548 shows absorption features in its X-ray and UV spectra. The large amount of optical/UV and X-ray monitoring data available for this object makes it an ideal candidate to test our model of a common X-ray/UV absorber. We show that the X-ray/UV absorption is caused by a highly ionized ($2.2 < U < 2.8$), high column density ($N_H = 3.8 \times 10^{21}$ cm$^{-2}$) gas situated outside the C IV emitting region ($2 \times 10^{16}$ cm $< r_{abs} < 2 \times 10^{18}$ cm). The gas is outflowing with a mean velocity of $1200 \pm 260$ km s$^{-1}$ and corresponding kinetic luminosity of $\sim 10^{43}$ ergs s$^{-1}$. The gas is more highly ionized and has a much larger column density than earlier estimates based on UV data alone. This third example of an X-ray/UV absorber reinforces our earlier conclusion that outflowing, highly ionized gas is common in the inner regions of quasars.

*Subject headings:* galaxies: individual (NGC 5548) — galaxies: active — galaxies: Seyfert — ultraviolet: galaxies — X-rays: galaxies

## 1. INTRODUCTION

Recently we found that the ionized ("warm") X-ray absorbers and the associated UV absorbers were due to the same material in two radio-loud quasars: an X-ray–quiet quasar, 3C 351 (Mathur et al. 1994), and a red quasar, 3C 212 (Mathur 1994). In both cases the absorber is situated outside the broad emission line region (BELR), is outflowing, and is highly ionized. While this result delineates a new nuclear component in lobe-dominated radio-loud quasars, it would clearly be much more interesting if the same component were present in all quasars and active galactic nuclei (AGNs) with both X-ray and UV absorption (Ulrich 1988). In this paper we test this generalization by applying the same model to the best studied of all AGNs, NGC 5548.

NGC 5548, a radio-quiet Seyfert 1 galaxy, provides the best test case for the equivalence of the X-ray and UV absorbers and will yield a highly constrained determination of the physical properties of the absorber. This is because NGC 5548 has been extensively studied in reverberation mapping experiments in the optical and UV (Peterson et al. 1992; Clavel et al. 1991; Korista et al. 1995). These have led to the accurate determination of the physical size of the BELR. NGC 5548 has both an X-ray–ionized absorber (Nandra et al. 1991; Fabian et al. 1994a) and an UV absorber (Shull & Sachs 1993), and the reverberation observations place limits on the response time of the UV absorbers to changes in the UV continuum. Note that this response time is due to the physical conditions of the absorber only, since there is no light-travel time delay along the line of sight.

We apply the photoionization modeling method of Mathur et al. (1994) to the X-ray and UV absorbers in NGC 5548 to determine whether consistent values for abundances of all the observed ions can be obtained. In NGC 5548 the model must meet two extra requirements: it must not lead to a density for the absorber in conflict with its recombination time; and the distance of the absorber from the continuum source must not conflict with the well-determined BELR size.

## 2. DATA

### 2.1. *X-Ray Data*

X-ray observations of NGC 5548 have revealed a complex spectrum. *EXOSAT* showed that the source has a strong soft excess (Branduardi-Raymont 1986, 1989). *Ginga* showed, moreover, that the X-ray spectrum and flux were variable (Nandra et al. 1991) and that the X-ray variability was correlated with the ultraviolet variability (Clavel et al. 1992). In addition, complex absorption was observed by *Ginga* with a possible Fe K edge at $\sim 8$ keV, corresponding to an intermediate ionization stage of ion ($\sim$Fe XX) with $\tau_{Fe\,K} \sim 0.03$ and variable soft X-ray absorption. *ROSAT* observations of NGC 5548 (1990 July 16–21) showed an absorption feature in its X-ray spectrum arising from highly ionized oxygen, demonstrating the presence of an ionized absorber; $E = 0.81 \pm 0.06$ keV, $\tau = 0.35 \pm 0.13$ (Nandra et al. 1993).

Recent observations with *ASCA* (1993 July 28) confirmed the presence of an ionized absorber (Fabian et al. 1994a). O VII and O VIII absorption edges observed at 0.72 keV and 0.86 keV, respectively, were resolved in the *ASCA* spectrum. The optical depths of the edges were $\tau_{O\,VII} = 0.26^{+0.04}_{-0.08}$ and $\tau_{O\,VIII} = 0.12^{+0.07}_{-0.03}$. The combined O VII and O VIII opacity from *ASCA* agrees well with that observed with *ROSAT*. An equivalent hydrogen column density was $N_H = 3.8 \times 10^{21}$ cm$^{-2}$. However, the presence of an Fe K edge is not confirmed ($\tau_{Fe\,K} \leq 0.1$).

The absorption cross sections of O VII and O VIII are $0.28 \times 10^{-18}$ cm$^2$ and $0.098 \times 10^{-18}$ cm$^2$, respectively (CLOUDY version 80.06; Ferland 1991). The column densities in the two ions are thus $N_{O\,VII} = 0.93^{+0.14}_{-0.29} \times 10^{18}$ cm$^{-2}$ and $N_{O\,VIII} = 1.22^{+0.72}_{-0.30} \times 10^{18}$ cm$^{-2}$. Given the total hydrogen column density and the solar abundance of oxygen relative to hydrogen ($=8.51 \times 10^{-4}$; Grevesse & Andres 1989) the fraction of oxygen in the two stages of ionization is calculated; $f_{O\,VII} = 0.29^{+0.04}_{-0.09}$ and $f_{O\,VIII} = 0.38^{+0.22}_{-0.10}$. The absorber must thus be highly ionized to have two-thirds of the oxygen in hydrogen-like and helium-like states.

### 2.2. *Ultraviolet Data: IUE*

NGC 5548 has been studied extensively in the ultraviolet (Clavel et al. 1991; Korista et al. 1995). The UV spectrum shows absorption lines of C IV and N V within the profiles of their broad emission lines (Shull & Sachs 1993, hereafter SS). The source was found to be highly variable in its continuum flux and also in the strengths of its emission and absorption lines. The UV continuum was found to vary by a factor of $\sim 3$, while the C IV absorption line equivalent width (EW) varied by a factor of $\sim 2$ over a period of about 10 days. There is no observed lag between the variations in the continuum and the EW of the C IV absorption line ($\Delta t \leq 4$ days; SS). Note that any delay between the continuum and absorption-line variability is *not* due to light-travel time (reverberation) effects, which are not operative along the line of sight. It is instead due to physical conditions within the absorber, specifically, the recombination time (see § 3.4). SS also infer a blueshift of $1200 \pm 260$ km s$^{-1}$ with respect to the systemic velocity of NGC 5548. We note that the earliest *IUE* spectra of NGC 5548 are also suggestive of an absorption feature at this position (Wu, Boggess, & Gull 1981; Ulrich & Boisson 1983). We reanalyzed the 1979 *IUE* data (SWP05500, SWP05687, SWP05688, SWP05689, SWP07345, SWP073930), including those reported by Wu et al. (1981) using current extraction techniques. The C IV absorption line is present at similar velocity and is of comparable strength to the later data (SS).

No associated Ly$\alpha$ absorption has been reported in the large literature on NGC 5548. Observationally it is difficult because the Ly$\alpha$ emission line of this low-redshift source lies very close to geocoronal Ly$\alpha$. Theoretically, Ly$\alpha$ absorption was not expected (SS), since the absorbing gas was considered "fully ionized" in hydrogen. As a result, all the published spectra cut off the blue wing of Ly$\alpha$ in the AGN emission line in order to remove geocoronal Ly$\alpha$ from the spectrum, cutting out also part of the Ly$\alpha$ absorption line.

Because our models predict significant Ly$\alpha$ absorption, we retrieved and reanalyzed a set of *IUE* spectra, taking care to go to shorter wavelengths. In Figure 1 we present an *IUE* spectrum of NGC 5548, without removing the geocoronal Ly$\alpha$. This clearly shows the presence of a Ly$\alpha$ absorption line at a redshift consistent with that of the other absorption lines.

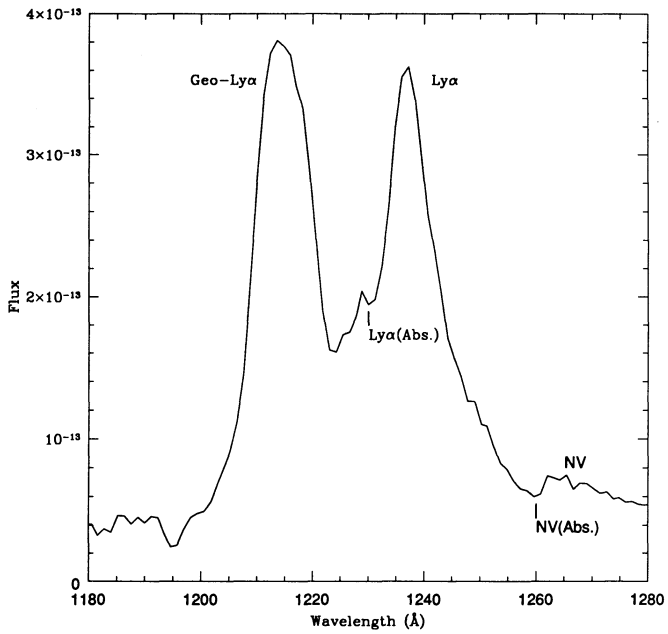


FIG. 1.—*IUE* spectrum of NGC 5548 (an average of SWP35029, SWP35284, SWP35461, SWP35636, SWP35849, SWP36018, SWP36369, SWP36567, and SWP36715) showing the presence of Ly$\alpha$ absorption line.

### 2.3. *Ultraviolet Data: Hubble Space Telescope*

NGC 5548 was observed daily for a total of 39 times by *HST* in 1993 April/May to monitor the variability of the source in the ultraviolet (1140 Å $< \lambda <$ 2312 Å; Korista et al. 1995). *HST* Faint Object Spectrograph (FOS) resolution is $\sim 1$ Å over this wavelength range (cf. $\sim 6$ Å with *IUE*). Figures 2*a* and 2*b* show the emission- and absorption-line profiles of Ly$\alpha$ and C IV, respectively, for the mean FOS spectrum. This spectrum was constructed by joining the combined G130H and G190H spectra; no scale factors were applied (see Korista et al. 1995, § 2.4). We measured the EWs of the absorption lines both in the individual *HST* spectra and in the mean. The C IV doublet $\lambda\lambda$1548, 1551 is resolved with EW $= 0.32 \pm 0.1$ and $0.08 \pm 0.03$ Å, respectively, in the mean FOS spectrum (Table


FIG. 2.—*HST* mean FOS spectrum of NGC 5548 showing (*a*) Ly$\alpha$, N V and (*b*) C IV absorption troughs. In (*a*) we also indicate our maximal and minimal estimates of the absorption-line strength (*dashed line*). The dotted line indicates the extrapolation to the observed line profile.

TABLE 1

ABSORPTION-LINE PARAMETERS

| LINE | $\lambda_{obs}$ (Å) | EW (Å) | |
|---|---|---|---|
| | | *HST*[a] | *IUE* |
| C IV λ1548.2..... | 1572.4 | 0.30 ± 0.10 | 1.6 ± 0.3[b] |
| C IV λ1550.8..... | 1575.4 | 0.08 ± 0.03 | |
| N V λ1238.8 ..... | 1260.7 | 0.04 ± 0.01 | ... |
| N V λ1242.8 ..... | 1262.5 | 0.10 ± 0.03 | |
| Lyα..... | 1234.1 | 0.5 ± 0.3 | ... |

[a] In mean spectrum.

[b] SS mean value scaled by our correction factor, 0.6 (see text).

1). The measurement of absorption lines situated within a broad emission line profile is notoriously difficult, since the real shape of the emission line is unknown. We estimated the magnitude of our errors by making maximal, minimal, and optimal measurements in each case (see, e.g., Fig. 2*a*). This yielded a typical error of about a factor of 2 in individual spectra and about 30% error in the mean FOS spectrum. The N V doublet is also resolved in the *HST* data with EW = 0.1 and 0.04 Å (±30%) in the mean spectrum.

An associated Lyα absorption line, at the same relative blueshift ($\Delta z = 0.002$) as the C IV–N V absorption system, is clearly seen with EW 0.5 ± 0.3 Å; a minimum H I column density is thus $N_{\rm H\,I} \geq 4 \times 10^{13}$ cm$^{-2}$. There is another absorption feature immediately shortward ($\lambda_{obs} = 1231.9$ Å, $\Delta z = 0.004$, EW ~ 0.6 Å). There are no corresponding C IV or N V absorption features at a similar relative blueshift, and the line appears to be unrelated to the associated absorption system we discuss here. The uncertainty in the Lyα EW is large owing to its proximity both to this nearby absorption feature and to the peak of the emission-line profile.

Note that the C IV EW in the mean *HST* spectrum is significantly lower than those reported for the *IUE* spectra (2 or 8 Å; SS) in 1989. The larger of the two SS EW values was derived by assuming that much of the emission-line peak was absorbed. This is clearly not the case in the higher resolution *HST* data. The *HST* spectra also show that the absorption feature covers a smaller range in wavelength than was apparent from the *IUE* data. We remeasured nine *IUE* spectra around JD 2,447,580, the time of the maximum continuum change, using $\Delta\lambda \sim 10$ Å, rather than the 16 Å used by SS. The exact wavelengths varied due to the inherent uncertainty in the wavelength calibration for spectra observed with the large *IUE* aperture. Our EW values are systematically smaller than SS's small values for the same spectra by a factor of 0.6. We used our revised measurements for the remainder of this paper. We note that the 1989 *IUE* C IV EWs are still larger than the *HST* values. This may be due to the measurement difficulties in the low-resolution *IUE* spectra.

## 3. MODELS

In the context of photoionization models we look for an ionized absorber that satisfies the X-ray constraints. Photoionization models predict the fraction of atoms in each ionization state, $f_{\rm ion}$, given the column density ($N_{\rm H}$), density ($n$), and ionization parameter $U$ [$U = (Q/4\pi r^2 n_{\rm H} c)$, where $Q$ is the number of ionizing photons] of a cloud of gas exposed to a continuum source with a defined continuum shape. All the photoionization calculations in this paper were performed using CLOUDY (Ferland 1991).

Mathur et al. (1994) have shown that the particular spectral energy distribution (SED) of each AGN should be used, rather than a "typical" quasar SED, since this might lead to incompatible physical conditions in a photoionized cloud. The observed radio to X-ray continuum of NGC 5548 is shown in Figure 3 (data from Ward et al. 1987; SS; Korista et al. 1995; Nandra et al. 1991). The continuum is corrected for Galactic reddening by $E(B-V) = 0.033$, assuming a fixed conversion of $N_{\rm H}/E(B-V) = 5.0 \times 10^{21}$ cm$^{-2}$ mag$^{-1}$ and $N_{\rm H}$ ($1.65 \times 10^{20}$ cm$^{-2}$; Nandra et al. 1993). The shape of the IR/optical continuum is similar to a typical AGN (Elvis et al. 1994) with the IR break shifted shortward to 100 μm. The standard radio-quiet AGN continuum used by Mathews & Ferland (1987) is shown for comparison as a dashed line. NGC 5548 is much brighter in X-rays than a typical AGN, but has a normal X-ray spectral slope, $\alpha_E = 0.8 \pm 0.2$ in the 2–10 keV range (Nandra et al. 1991). In addition, it has a soft X-ray excess which can be approximated by a blackbody spectrum of temperature 150,000 K (Fig. 3, *dotted line*). The heavy solid line in Figure 3 shows the adopted input continuum. The X-ray column density $N_{\rm H}$ was fixed at the observed *ASCA* value of $3.8 \times 10^{21}$ cm$^{-2}$ (Fabian et al. 1994a).

### 3.1. *The X-Ray Absorber*

Figure 4 shows the ionization fractions of O VII and O VIII as a function of $U$, using the dereddened continuum for NGC 5548 and assuming solar abundances (Grevesse & Andres 1989). The number of ionizing photons $Q$ is equal to $2.5\ h_{50}^{-2} \times 10^{54}$ s$^{-1}$, where $h_{50}$ is the Hubble constant in units of 50 km s$^{-1}$ Mpc$^{-1}$. Note that this value of $Q$ is in fact smaller than that used by Ferland et al. (1992), $Q = 4\ h^{-2} \times 10^{54}$ s$^{-1}$, which is based on a scaled version of the standard continuum. This is because most of the ionizing photons come from the energy range 1–20 rydbergs, where the standard continuum is brighter (Fig. 3). The observed values are highlighted with heavy lines. Using the constraints on the fractional ionization of O VII and O VIII from the *ASCA* data ($\tau_{\rm O\,VII} = 0.29^{+0.04}_{-0.09}$, $\tau_{\rm O\,VIII} = 0.38^{+0.22}_{-0.09}$; Fabian et al. 1994a; see § 2.1 above), the allowed

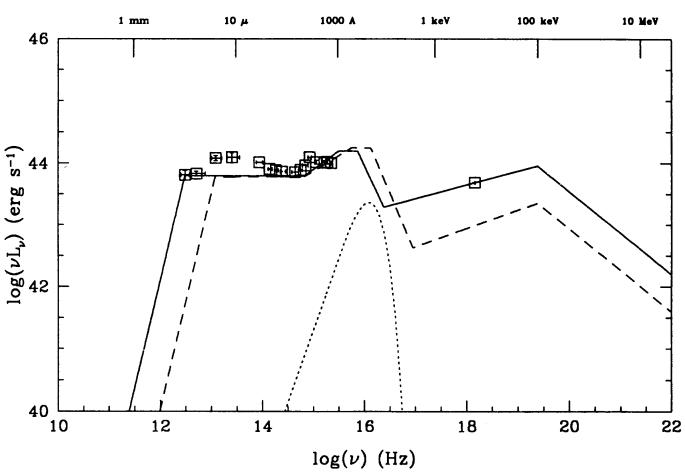


FIG. 3.—Spectral energy distribution of NGC 5548: the data are from Ward et al. (1987), SS, and Nandra et al. (1991). The solid line represents our adopted SED. The dotted line is a 150,000 K blackbody spectrum. The dashed line is a "standard" AGN continuum shown for comparison (see text).

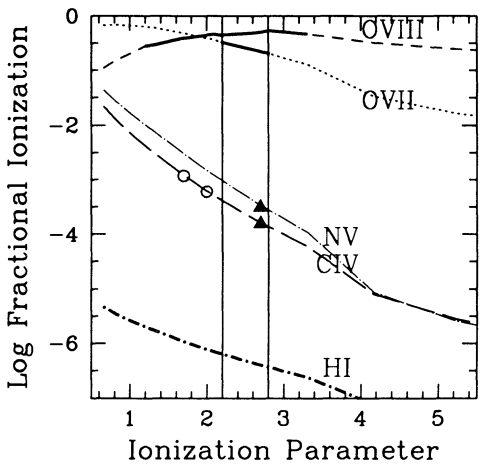


FIG. 4.—Ionization fractions of O VII, O VIII, C IV, N V, and H I as a function of $U$. The heavy lines mark the observed ranges for O VII and O VIII (*ASCA*). *Triangles HST* values for C IV and N V; *circles IUE* range. The *HST* range for H I is large (see text), represented by the heavy curve. The vertical lines define the best-fit model parameter: $2.2 < U < 2.8$.

range of the ionization parameter is narrow, $2.2 < U < 2.8$. (Note that this is a *linear* scale.) If instead the observed continuum is used, i.e., with no reddening correction, the inferred range changes to $1.2 < U < 1.3$ and the dependence of $\log f_{\rm ion}$ on $U$ remains qualitatively the same. In the rest of the paper we quote all the parameters only for the reddening-corrected SED. The values of the ionization fraction are independent of the gas density, so the density $n$ is not constrained by photoionization models alone (see § 3.4). The value $n = 10^7$ atoms cm$^{-3}$ was used in the input to CLOUDY.

We investigated whether the lack of an Fe K absorption feature observed by *ASCA* (§ 2.1) is consistent with our model. The ~8 keV Fe K absorption edge would most likely be due to an intermediate ionization stage of ion around Fe XX (Nandra et al. 1991), most likely Fe XVII, since it dominates over a wider range of $U$ than other ionization states because it is neon-like and so more stable than other iron ions.

We find that, for the best-fit models for the oxygen edges, the dominant stage of iron is indeed Fe XVII, $\log f_{\rm Fe\,XVII} = -0.77$, implying $N_{\rm Fe\,XVII} < 2.2 \times 10^{18}$ cm$^{-2}$. The *ASCA* upper limit to an Fe K edge is $\tau < 0.1$ (§ 2.1), so $N_{\rm Fe\,XVII} = 3 \times 10^{16}$ cm$^{-2}$, assuming solar abundance of iron ($4.68 \times 10^{-5}$; Grevesse & Andres 1989). This is consistent with the absence of any Fe K X-ray absorption edges. This absorption system, however, falls short by a factor of ~25 of producing the large observed EW of the Fe K emission line even for a uniform spherical shell (model EW ~7 eV, observed EW = 180 ± 60 eV), consistent with the conclusion of Nandra et al. (1991).

### 3.2. *Combined X-Ray and Ultraviolet Constraints*

We follow the technique developed in Mathur et al. (1994) to look for an absorption system that satisfies both X-ray and UV constraints. The X-ray constraints require $2.2 < U < 2.8$, as discussed above. Thus, if the X-ray and UV absorbers are one and the same (as was found to be the case in 3C 351 and 3C 212) in NGC 5548, then it can be seen from Figure 4 that the ionization fraction of C IV is constrained to be $f_{\rm C\,IV} = 2.0^{+0.5}_{-0.4} \times 10^{-4}$ ($\log f_{\rm C\,IV} = -3.7^{+0.2}_{-0.3}$).

In the mean *HST* spectrum, the C IV doublet ratio is 3.8 ± 0.2; thus the C IV absorption lines lie off the linear portion of the curve of growth (see, e.g., Spitzer 1978; Wiese et al. 1966). In Figures 5*a*–5*c* the curves of growth for velocity spread parameters $b$ = 20, 40, 60, and 80 km s$^{-1}$ are shown. Figure 5*a* shows the observed equivalent width for C IV (Table 2) and the constraint on $\log (Nf\lambda)$ derived from the X-ray constraint on $f_{\rm C\,IV}$ (see above) assuming a solar abundance for carbon ($3.63 \times 10^{-4}$; Grevesse & Andres 1989) and oscillator strength $f = 0.285$ (Allen 1973). Similar plots (Figs. 5*b* and 5*c*) for N V (at solar abundance, $3.63 \times 10^{-4}$; Grevesse & Andres 1989) and Lyα (using oscillator strengths of 0.235 and 0.4162 for N V and Lyα, respectively; Allen 1973) lead to the allowed $b$-values given in Table 2. A consistent solution for all three ions is obtained for $b$ = 40 km s$^{-1}$, with a small tolerance for both UV and X-ray constraints to be met.

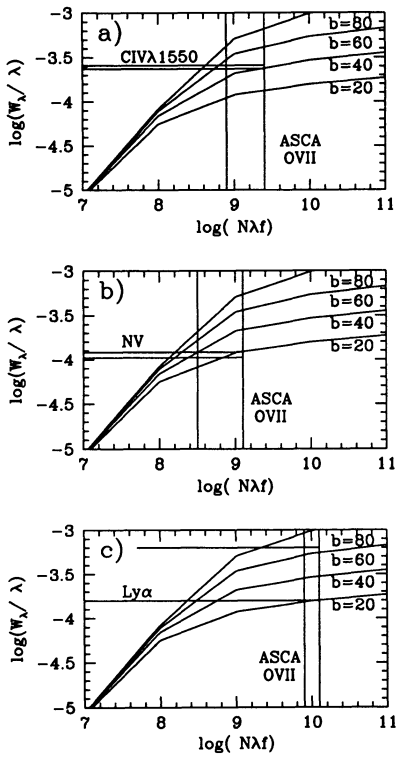


FIG. 5.—Curve of growth for $b$-values from 20 to 80 km s$^{-1}$ in steps of 20 km s$^{-1}$. Horizontal lines are for the observed values of absorption lines in the mean *HST* spectrum. (*a*) C IV; (*b*) N V ; and (*c*) Lyα.

The measured line widths for the C IV doublet are ~350 km s$^{-1}$ (FWHM), broader than the nominal spectral resolution for this observation and thus possibly resolved. This would imply that the absorber is dispersed in velocity space (see also SS). However, we note that the resolution of the FOS using the 4″.3 slit (as in the case) is not well defined. In particular, ~50% of the light is in very broad wings (K. Korista 1995, private communication), and thus we cannot be certain that the line is

TABLE 2

UV AND X-RAY CONSTRAINTS ON $b$[a]

| Ion | $\log (W_\lambda/\lambda)$ (from UV) | $\log (N\lambda f)$ (from X-Ray) | $b$ (km s$^{-1}$) |
|---|---|---|---|
| C IV..... | $-3.61 \pm 0.02$ | 8.9–9.4 | 40–50 |
| N V ..... | $-3.92 \pm 0.03$ | 8.5–9.1 | 18–40 |
| H I..... | $-3.8^{+0.3}_{-0.2}$ | 9.9–10.1 | 20–60 |

[a] Ranges are ± 1 σ.

resolved from these data. As discussed in § 2.3, the uncertainty in the Lyα EW is large, leading to a large uncertainty in the H I column density: $13 < \log N_{\rm H\,I} < 18$, while the model value ranges from 15.2 to 15.4 (Table 2). An actual H I column density in the higher end of the observed range would imply that the heavy-element abundance in the X-ray/UV absorber is depleted. Conversely, if it is in the lower end of the range, enhanced metal abundance is implied. A Lyman edge absorption would be observed if $N_{\rm H\,I}$ is large ($\log N_{\rm H\,I} > 16.3$). The recent HUT observations (1995 spring) will be able to detect such a Lyman edge.

The *ASCA* observations were made on 1993 July 28, while the *HST* observations were made between 1993 April and 1993 May. The close agreement of $U$ from the *ASCA* and *HST* data requires that the UV continuum flux be similar in both observations. The optical light curve of NGC 5548 (Korista et al. 1995) shows that the mean continuum level during the *HST* observations [$f_\lambda(5100\ \text{Å}) = 9.14 \times 10^{-15}$ ergs s$^{-1}$ cm$^{-2}$ Å$^{-1}$] was indeed only 4% below the continuum at the time of the *ASCA* observations ($\sim 9.4 \times 10^{-15}$ ergs s$^{-1}$ cm$^{-2}$ Å$^{-1}$).

One additional consistency check is possible. In a highly ionized system such as this, magnesium is highly ionized (Mg VI and higher), leaving no magnesium in the Mg II state (log $f_{\rm Mg\,II} < -30$), and thus Mg II absorption should not occur. This is consistent with the observations (§ 2.2).

Thus we have a single consistent model that simultaneously, correctly predicts the fractional ionization of O VII, O VIII, N V, C IV, H I, and Fe XVII and the lack of presence of Mg II and other low-ionization species. We conclude that the UV and X-ray absorbers in NGC 5548 are one and the same.

### 3.3. *Variability*

Our photoionization model of the UV absorber in NGC 5548 must explain the observed variability of the C IV absorption line (SS), assuming that their relative measurements are correct (see § 2.3). As can be seen from Figure 5, the absorption line lies slightly off the linear part of the curve of growth. The slope of the curve of growth in that region is about 0.5. Since this is a log-log plot, a factor of 2 change in the column density of the C IV ion would result in a factor of 1.4 change in the EW of the line. In our model, the variations in $N_{\rm ion}$ are caused by variations in the ionization parameter of the absorber (Fig. 4), which is directly proportional to the variations in the ionizing flux. An increase in $U$ results in a decrease in $N_{\rm C\,IV}$ (Fig. 4). Our measurements of the *IUE* data show the continuum at 1500 Å varying from $2.0 \times 10^{-14}$ to $4.7 \times 10^{-14}$ ergs cm$^{-2}$ s$^{-1}$ Å$^{-1}$, a factor of 2.4, while the C IV absorption-line EW changes from $1.9 \pm 0.3$ to $1.4 \pm 0.4$ Å, consistent with the model prediction of a factor of 1.5.

During the *HST* observations the maximum continuum variations were only a factor of $\sim 1.5$ (Fig. 6). There is no obvious variability observed in the C IV absorption line EW. Unfortunately, the errors in the C IV EW are large, owing to the inherent measurement difficulty discussed earlier (§ 2.3). The two solid lines indicate the variability predicted by our model based on the observed continuum variations and both zero time lag and a time lag of 2 days. The data are certainly consistent with the model ($\chi^2 = 6.05$ for 35 degrees of freedom); however, no strong conclusions can be drawn.

### 3.4. *Physical Properties of the Absorber*

The X-ray/UV absorber in NGC 5548 shows absorption features due to Lyα, N V, C IV, O VII, O VIII, and Fe XVII. The

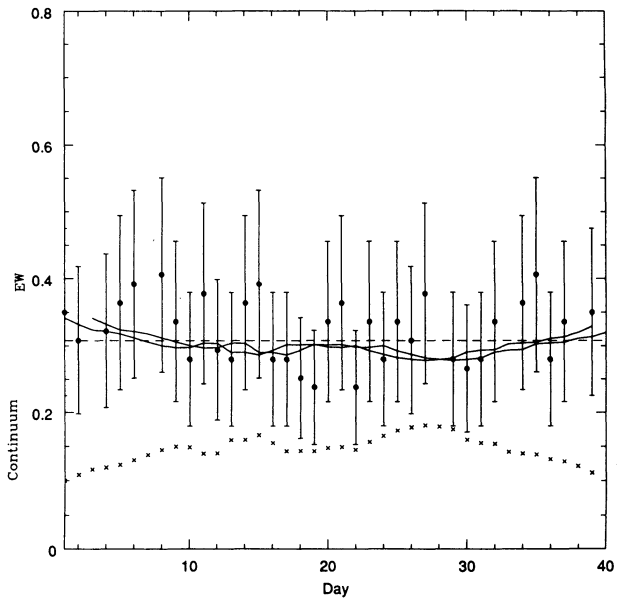


FIG. 6.—Variability in the continuum and C IV absorption-line EW during *HST* observations. The continuum is in arbitrary units. The dashed horizontal line is the mean EW. The two solid lines represent the predicted variability for no time lag and for a time lag of 2 days.

X-ray and UV constraints can now be combined to derive the physical properties of the absorber. It is highly ionized ($2.2 < U < 2.8$) and has a large column density ($N_{\rm H} = 3.8 \times 10^{21}$ cm$^{-2}$). The C IV recombination time must be shorter than the variability response timescale of $\lesssim 4$ days (SS), which sets a lower limit to the density of the absorber; $n \gtrsim 5 \times 10^5\ t_4^{-1}$ cm$^{-3}$, where $t_4$ is the lag between the continuum and absorption-line variation in units of 4 days. The thickness of the absorbing slab is then $\Delta r \lesssim 8 \times 10^{15}$ cm. It is outflowing with a mean velocity of $v_{\rm out} = 1200 \pm 260$ km s$^{-1}$, as inferred by its blueshift with respect to the systemic velocity of the galaxy (SS) and possibly dispersed in velocity (FWHM $\sim 300$ km s$^{-1}$).

The radial distance of the absorber, $r_{\rm abs} = (Q/4\pi U n_{\rm H} c)^{1/2}$, is $\lesssim 0.7$–$0.8\ t_4^{1/2}$ pc, given the above density constraint. The maximum depth of the C IV absorption line during the *IUE* observations is greater than the continuum level (SS). This implies that the absorber at least partially covers the C IV emitting region, whose size has been accurately determined for NGC 5548 as $7.5 \pm 0.5$ lt-days. Combining these two limits gives 8 lt-days $< r_{\rm abs} < 0.8$ pc, i.e., $2 \times 10^{16} < r_{\rm abs} < 2 \times 10^{18}$ cm.

The lower limit on $r_{\rm abs}$ limits the density to $n < 5 \times 10^9$ cm$^{-3}$. The density is thus constrained to be $5 \times 10^5\ t_4^{-1} < n < 5 \times 10^9$ cm$^{-3}$. The radial distance and density are not strongly constrained, nor are the model constraints in conflict with those from the variability data.

Associated absorption has been observed in $\sim 10\%$ of Seyfert 1 galaxies (Ulrich 1988), which implies a $\sim 10\%$ covering factor of the absorber in all Seyfert 1 galaxies. If we assume that this covering factor, $f_{0.1}$, applies to NGC 5548, then the mass of the absorber is $M_{\rm abs} \sim 20 f_{0.1}\ M_\odot$. The mass outflow rate can be calculated, by assuming uniform density: $\dot{M}_{\rm out} = M_{\rm abs} v_{\rm out} \Delta r^{-1} f_{0.1} = 10 f_{0.1}\ M_\odot$ yr$^{-1}$. This is an upper limit in that the absorber is much thinner than its radius from the

TABLE 3

PHYSICAL CONDITIONS OF X-RAY/UV ABSORBER

| Parameter | Constraint | Derived from: |
|---|---|---|
| Neutral hydrogen column density $N_H$..... | $N_H \sim 3.8 \times 10^{21}$ cm$^{-2}$ | X-ray (Fabian et al. 1994a) |
| Ionization parameter $U$..... | $2.2 < U < 2.8$ | $\tau$(O VII, O VIII), X-ray (Fabian et al. 1994a; Nandra et al. 1993) |
| Radial distance $r_{abs}$..... | $2 \times 10^{16}$ cm $< r_{abs} < 2 \times 10^{18}$ cm | LL: BELR covered (Peterson et al. 1992); UL: $n$, $U$ |
| Density $n$..... | $5 \times 10^5$ cm$^{-3} \lesssim n < 5 \times 10^9$ cm$^{-3}$ | LL: recombination time $< 4$ days (SS); UL: $r_{abs}$, $U$ |
| Outflow velocity $v$..... | $1200 \pm 260$ km s$^{-1}$ | Line redshift (SS) |
| Thickness $\Delta r$..... | $\lesssim 8 \times 10^{15}$ cm | $N_H$, $n$ |
| Mass..... | $\sim 20 f_{0.1} M_\odot$ | $n$, $r_{abs}$, $\Delta r$ (covering factor $f_{0.1} = 0.1$) |

center, so that the time-averaged $\dot{M}_{out}$ is likely to be much smaller. The same rate is a lower limit in that we measure only the velocity component in our line of sight (see § 4.4). This mass outflow rate is quite a bit larger than the accretion rate of 0.08 $M_\odot$ yr$^{-1}$ needed to power the $L_{bol} = 5 \times 10^{44}$ ergs s$^{-1}$ continuum source at 10% efficiency. The outflow would carry a kinetic luminosity of $\dot{M}_{out}^2 v_{out}^2/2 = \sim 10^{43}$ ergs s$^{-1}$ about 50 times lower than the radiative luminosity of NGC 5548. A summary of the properties of the absorber is given in Table 3.

## 4. DISCUSSION

### 4.1. *Comparison with Previous Models*

The combination of X-ray and improved UV constraints from *HST* have led to derived conditions very different from those reported earlier by SS based on the *IUE* data alone. SS necessarily assumed C IV to be the dominant state of ionization ($f_{C\,IV} = 0.1$), leading to $U \sim 10^{-3}$. Combining this with the lack of Mg II absorption led to $N_H < 10^{20.5}$ cm$^{-2}$. However, in our model these parameters are constrained: $2.2 < U < 2.6$, $-3.4 < f_{C\,IV} < -3.9$. We are thus led to conclude that the absorber is highly ionized and has a large column density ($N_H = 3.8 \times 10^{21}$ cm$^{-2}$; Fabian et al. 1994a).

### 4.2. *Generalizing X-Ray/Ultraviolet Absorbing Outflows*

The physical properties of the long-known UV absorber in NGC 5548 are now well constrained with the identification of an X-ray/UV absorber. We can therefore generalize our unification of X-ray and UV absorbing outflows for lobe-dominated radio-loud quasars to include radio-quiet Seyfert galaxies, and most likely to include all associated absorbers in AGNs.

A strong correlation has been observed between the radio properties and associated absorption-line properties of AGNs: all broad absorption line quasars (BALQSOs) are radio-quiet (Stocke et al. 1992), and all Mg II associated absorption-line quasars are lobe-dominated and radio-loud (Aldcroft, Elvis, & Bechtold 1995). Associated C IV absorbers are a mixture of lobe- and core-dominated radio-loud quasars, and radio-quiet quasars. It is of interest to note that even though NGC 5548 is radio-quiet, it is unusual in that its radio luminosity is dominated by the extended radio flux, which has a larger physical size than in any other radio-quiet Seyfert galaxy (Wilson & Ulvestad 1982). In this respect it is similar to a lobe-dominated quasar, providing a link between lobe-dominated, radio-loud AGNs with associated absorption and radio-quiet AGNs, perhaps also the BALQSOs. It further suggests that AGNs with X-ray/UV absorbers are edge-on. To have an inclination indicator in radio-quiet AGNs would be most valuable, and this possibility should be studied further.

### 4.3. *Comments on Variability in NGC 3227 and MCG −6-30-15*

Variable X-ray spectra and the existence of ionized absorbers have been observed with *ASCA* in two more AGNs: NGC 3227 (Ptak et al. 1994) and MCG −6-30-15 (Fabian et al. 1994b). In both cases the variations in the properties of the ionized absorbers were deduced to be incompatible with the variations seen in the continuum.

In NGC 3227 (Ptak et al. 1994) rapid flux variations were observed with a timescale of $\sim 10^4$ s. An O VI absorption edge was detected with opacity $\tau \sim 0.75$. The model fits to the spectra in high- and low-flux states showed that (1) for the same value of photon index $\Gamma$ in both high and low states, $N_H$ and $U$ *decrease* when the luminosity increases; (2) for different values of $\Gamma$, the same $N_H$ and $U$ can be fitted in both high and low states. Both of these models seem unphysical, and hence the authors suggested that a warm absorber model may be too simple.

This however, may not be the case, since it does not allow for delays due to the recombination time of the absorber. The best-fit $\tau$ in NGC 3227 is remarkably similar in both high and low states, implying that the ionization structure of the absorber has not changed even though the luminosity has changed. This implies a recombination time of O VI $> 10^4$ s. For O VI the recombination time is $T = 4.3 \times 10^4 n_6^{-1}$ s (Shull & Van Steenberg 1982), where $n_6$ is the density in the units of $10^6$ cm$^{-3}$. This implies a density of the warm absorber, $n < 10^6$ cm$^{-3}$. With the model value of $U$ is of order 0.05, this places the absorber at $r = 10^{19}$ cm, well outside the BELR (which would have a radius of $7 \times 10^{15}$ cm, assuming an $L^{1/2}$ scaling from NGC 5548).

It should be noted that the physical parameter which responds to continuum variations is $\tau$ rather than $U$. Indeed, if $\tau$ remains the same while the luminosity increases, the fitted value of $U$, which assumes the system is in equilibrium, would necessarily decrease.

A similar apparent discrepancy was observed in MCG −6-30-15 (Fabian et al. 1994b) which has an O VII absorption edge. In this case $\tau$ decreased significantly over 23 days. The luminosity also decreased over this period, while the fitted value of the ionization parameter increased. Whether the change in $\tau$ correlates or anticorrelates with the change in luminosity depends upon $U$ (see Fig. 4). The recombination time of O VII is $\sim 0.28 n_6^{-1}$ days (Shull & Van Steenberg 1982). The data imply that $t \leq 23$ days and so $n \geq 10^4$ cm$^{-3}$, a very reasonable constraint.

We argue that the warm absorber models in NGC 3227 and MCG −6-30-15 are *not* unphysical and that the data do not require more complex models. The information provided by the variability not only helps us understand this fact but also

provides an important constraint on the density of the absorber.

The low value of $U$ for NGC 3227 (cf. $U = 2.6$ for NGC 5548) implies a wide range of ionization states from object to object for the associated absorbers in radio-quiet AGNs as in radio-loud.

### 4.4. *Implications for the Nature of the Outflowing Material*

Now that we understand the physical properties of the absorber, we can begin to ask astrophysical questions.

The lack of differential time delays between the red and blue wings of the broad-line profiles shows that the BELR motions are not primarily radial (Korista et al. 1995). Yet the absorbing material outside the BELR shows large outflows, both in NGC 5548 and in the other UV absorbers (Ulrich 1988). How is the orbital or random motion at BELR radii converted to an organized flow? What is the driving force? The continuum radiation pressure acting on the partially ionized gas (Mathur et al. 1994; Turner et al. 1994) may play an important role. In a more specific scenario, Glenn, Schmidt, & Foltz (1994) and Aldcroft et al. (1995) have independently suggested that in BALQSOs and radio-loud quasars, respectively, we are looking almost edge-on at material blown off a dusty disk (which itself may be the BELR) by radiation pressure. Since there is some evidence that NGC 5548 too is edge-on, the same picture may apply there.

Material escaping vertically from an edge-on disk would then follow a path that is not purely radial, since it is accelerated by the continuum radiation pressure. If the material originates at only a restricted range of radii in the disk, this could explain a number of otherwise puzzling features. In particular, the limited thickness of the absorber in NGC 5548 cannot be understood in any continuous radial wind model. The X-ray column density directly rules out significant additional accelerated or decelerated material, unless it is fully stripped through iron (Nandra et al. 1991). Only by making the wind intermittent, or by allowing for a velocity component in the plane of the sky (so moving the rest of the flow out of our line of sight), can we keep the thickness small.

Another consistency check is to confirm that the persistence of the absorber is consistent with the large observed outflow velocity ($1200 \pm 200$ km s$^{-1}$). In the 3 years separating the *ROSAT* and *ASCA* observations, no significant change in the O VII/O VIII opacity was detected. (*ROSAT* $\tau = 0.35 \pm 0.13$ [Nandra et al. 1993]; *ASCA* $\tau = 0.38^{+0.08}_{-0.09}$ [Fabian et al. 1994a]). A formal 3 $\sigma$ upper limit for a change in $\tau$ is 0.27 (i.e., $\sim$80%). The distance traveled by the absorber in 3 yr is $1.2 \times 10^{16}$ cm. In order to limit a change in $U$ to less than 80%, this must represent less than a 34% change in distance from the ionizing continuum (assuming a constant-density system). This leads to $r_{\rm abs} \geq 3.5 \times 10^{16}$ cm, slightly larger than the minimum distance determined from the size of the BELR ($2 \times 10^{16}$ cm; § 3.4) and so consistent with our earlier derived parameters for the absorber.

The first *IUE* observations, some 15 years ago, also showed a C IV absorber at a similar velocity and depth (§ 2.2). These observations provide more constraints. The outflow cannot be intermittent if it has persisted for 15 yr. Assuming a constant mean velocity for the absorber leads to a present minimum distance $r_{\rm abs} > 5 \times 10^{16}$ cm, and a corresponding maximum density $n < 8 \times 10^8$ cm$^{-3}$. These are both consistent with the derived absorber parameters (§ 3.4). However, if the apparent width of the absorption line in the *HST* data is real ($\sim$300 km s$^{-1}$) and represents the internal velocity dispersion of the gas over the past 15 yr, then it will have led to a thickening by $\sim 10^{16}$ cm over 15 yr, comparable to our estimate of the present absorber thickness (less than $8 \times 10^{15}$ cm; § 3.4). In this case the absorber would have had zero depth when *IUE* first observed it, which is unlikely, since otherwise it has not changed significantly. This difficulty disappears if we are looking through a flow with a component in the plane of the sky, since then we are seeing a steady state flow crossing our path. This dynamical picture, derived from observations, is similar to the model of broad absorption line quasars (BALQSOs) by Murray et al. (1995).

Testing the model further in NGC 5548 could be achieved by measuring the recombination time, and hence the absorber density. This implies a small sampling interval (less than 1 day) accompanied by continuum changes by at least a factor of 2. Monitoring the ionization parameter at a given continuum flux over a number of years to search for density changes would also test the model. High spectral resolution observations (e.g., with the *HST* Goddard High-Resolution Spectrograph) could examine the velocity structure of the absorber, and perhaps measure $b$-values of any components. Tests for the edge-on nature of AGNs with X-ray/UV absorbers also need to be pursued.

## 5. CONCLUSIONS

In this paper we have shown that the X-ray and UV absorption in NGC 5548 can be explained quantitatively by having the same material produce the absorption features due to O VII, O VIII (in X-rays), C IV, N V, and H I (in the UV), and not produce observable features due to Fe XVII and Mg II and other low-ionization lines. This simple model passes further tests by not violating the size and density limits imposed by the reverberation mapping data. We conclude that the X-ray and the UV absorption do indeed arise from the same material.

Combining the improved X-ray and UV constraints from *ASCA* and *HST*, together with the reverberation mapping variability constraints, leads us to understand the physical properties of the absorber. The absorber is highly ionized ($2.2 < U < 2.8$), has high column density ($N_{\rm H} = 3.8 \times 10^{21}$ cm$^{-2}$), low density ($5 \times 10^5\ t_4^{-1} < n < 5 \times 10^9$ cm$^{-3}$), and is situated outside the C IV emitting region ($2 \times 10^{16} < r_{\rm abs} < 2 \times 10^{18}$ cm). The gas is outflowing with a mean velocity of $1200 \pm 200$ km s$^{-1}$ and has a corresponding kinetic luminosity of $\sim 10^{43}$ ergs s$^{-1}$.

We can now generalize our unification of UV and X-ray absorbing outflows from the lobe-dominated radio-loud quasars to include radio-quiet Seyfert galaxies. This may also provide a link to the radio-quiet BALQSOs. This analogy suggests that the X-ray/UV absorbers in radio-quiet AGNs may be viewed close to edge-on, which would be a valuable known parameter if it can be independently supported. Now that we understand the physical properties of the absorber, we can begin to ask astrophysical questions about the dynamics of the outflow and its role in the circumnuclear region of AGNs. A scenario in which the absorbing material comes off a disk and is accelerated by the radiation pressure of the continuum source may explain the persistence of the absorber in spite of its large velocity and thin shell-like geometry.

We thank Brad Peterson and Kirk Korista for valuable discussions and for early access to the *HST* spectra. We also thank Jonathan McDowell for his TIGER software. This work was supported in part by NASA grant NAGW5-2201 (LTSA), and NASA contracts NAS8-39073 (ASC), NAS5-30934 (RSDC).

REFERENCES

Aldcroft, T., Elvis, M., & Bechtold, J. 1995, MNRAS, submitted
Allen, C. W. 1973, Astrophysical Quantities (London: Athlone)
Branduardi-Raymont, G. 1986, in The Physics of Accretion onto Compct Objects, ed. K. O. Mason, M. G. Watson, & N. E. White (Berlin: Springer), 407
———. 1989, in Active Galactic Nuclei, ed. D. E. Osterbrock & J. S. Miller (Dordrecht: Kluwer), 177
Clavel, J., et al. 1991, ApJ, 366, 64
———. 1992, ApJ, 393, 113
Elvis, M., et al. 1994, ApJS, 95, 1
Fabian, A., Nandra, K., Brandt, W., Hayashida, K., Makino, F., & Yamauchi, M. 1994a, in New Horizons in X-Ray Astronomy, ed. F. Makino & T. Ohashi (Tokyo: Universal Academy Press), 573
Fabian, A., et al. 1994b, PASJ, 46, L59
Ferland, G. F. 1991, "HAZY": OSU Astronomy Dept. Internal Rep.
Ferland, G. F., Peterson, B., Horne, K., Welsh, W. F., & Nahar, S. N. 1992, ApJ, 387, 95
Glenn, J., Schmidt, G., & Foltz, C. 1994, ApJ, 434, L47
Grevesse, N., & Andres, E. 1989, in AIP Conf. Proc. 183, Cosmic Abundances of Matter, ed. C. J. Waddington (New York: AIP)
Korista, K., et al. 1995, ApJS, 97, 285
Mathews, W. G., & Ferland, G. J. 1987, ApJ, 323, 456
Mathur, S. 1994, ApJ, 431, L75
Mathur, S., Wilkes, B., Elvis, M., & Fiore, F. 1994, ApJ, 434, 493
Murray, N., Chiang, J., Grossman, S. A., & Voit, G. M. 1995, ApJ, in press
Nandra, K., et al. 1991, MNRAS, 248, 760
———. 1993, MNRAS, 260, 504
Peterson, B. M., et al. 1992, ApJ, 392, 470
Ptak, A., Yaqoob, T., Serlemitsos, P. J., Mushotzky, R., & Otani, C. 1994, ApJ, 436, 31
Shull, M. J., & Sachs, E. R. 1993, ApJ, 416, 536 (SS)
Shull, M. J., & Van Steenberg, M. E. 1982, ApJS, 48, 95
Spitzer, L. 1978, Physical Processes in the Interstellar Medium (New York: Wiley-Interscience), 46
Stocke, J. T., Morris, S. L., Weymann, R. J., & Foltz, C. B. 1992, ApJ, 396, 487
Turner, T. J., Nandra, K., George, I. M., Fabian, A., & Pounds, K. A. 1994, ApJ, 419, 127
Ulrich, M. H. 1988, MNRAS, 230, 121
Ulrich, M. H., & Boisson, C. 1983, ApJ, 267, 515
Ward, M., Elvis, M., Fabbiano, G., Carleton, N. P., Willner, S. P., & Lawrence, A. 1987, ApJ, 315, 74
Wiese, W. L., Smith, M. W., & Glennon, B. M. 1966, Atomic Transition Probabilities (Washington, DC: GPO)
Wilson, A., & Ulvestad, J. 1982, ApJ, 263, 576
Wu, C., Boggess, A., & Gull, T. 1981, ApJ, 247, 449